HHS Public Access

Author manuscript

Cell Rep. Author manuscript; available in PMC 2017 December 20.

Published in final edited form as:

Cell Rep. 2016 December 20; 17(12): 3115–3124. doi:10.1016/j.celrep.2016.11.067.

Beyond Epilepsy and Autism: Disruption of *GABRB3* Causes Ocular Hypopigmentation

Ryan J. Delahanty[1,2], **Yanfeng Zhang**[1], **Terry Jo Bichell**[3], **Wangzhen Shen**[3], **Kelienne Verdier**[3], **Robert L. Macdonald**[3,4,5,6], **Lili Xu**[3], **Kelli Boyd**[7], **Janice Williams**[8], and **Jing-Qiong Kang**[3,6,9,*]

[1]Division of Epidemiology, Department of Medicine, Vanderbilt University Medical Center, Nashville, TN 37212

[2]Department of Human Genetics, Vanderbilt University Medical Center, Nashville, TN 37212

[3]Department of Neurology, Vanderbilt University Medical Center, Nashville, TN 37212

[4]Department of Molecular Physiology and Biophysics, Vanderbilt University Medical Center, Nashville, TN 37212

[5]Department of Pharmacology, Vanderbilt University Medical Center, Nashville, TN 37212

[6]Vanderbilt Brain Institute, Vanderbilt University Medical Center, Nashville, TN 37212

[7]Pathology Microbiology and Immunology, Vanderbilt University Medical Center, Nashville, TN 37212

[8]Vanderbilt Electron Microscopy Core, Vanderbilt University Medical Center, Nashville, TN 37212

Abstract

Reduced ocular pigmentation is common in Angelman syndrome (AS) and Prader-Willi syndrome (PWS) and long thought to be caused by *OCA2* deletion. *GABRB3* is located in the 15q11-13 region flanked by *UBE3A, GABRA5, GABRG3* and *OCA2*. Mutations in *GABRB3* have been frequently associated with epilepsy and autism, consistent with its role in neurodevelopment. We report here a robust phenotype in the mouse in which deletion of *Gabrb3* alone causes nearly complete loss of retinal pigmentation due to atrophied melanosomes, as evidenced by electron microscopy. Using exome and RNA sequencing, we confirmed that only the *Gabrb3* gene was disrupted while the *Oca2* gene was intact. However, mRNA abundance of *Oca2* and other genes adjacent to *Gabrb3* is substantially reduced in *Gabrb3*$^{-/-}$ mice, suggesting complex transcriptional

[*]**Corresponding Author**: Jing-Qiong Kang, M.D, Ph.D., Vanderbilt University Medical Center, 6140 Medical Research Building III, 465 21st Ave, South Nashville, TN 37232-8552, Tel: 615-936-8399; fax: 615-322-5517, jingqiong.kang@vanderbilt.edu.
[9]lead contact

Author Contributions: RD and YZ analyzed data. TB collected the human eye images and edited paper. WS collected data. KV helped on colony maintenance and genotyping. RLM edited paper. LX provided advice on eye sample preparation. KB consulted on mouse eye anatomy. JW helped collect data. JQK designed the project, performed experiments; analyzed the data and supervised the project. RD and JQK wrote the manuscript.

regulation in this region. These results suggest that impairment in *GABRB3* downregulates *OCA2* and indirectly causes ocular hypopigmentation and visual defects in AS and PWS.

Graphical abstract

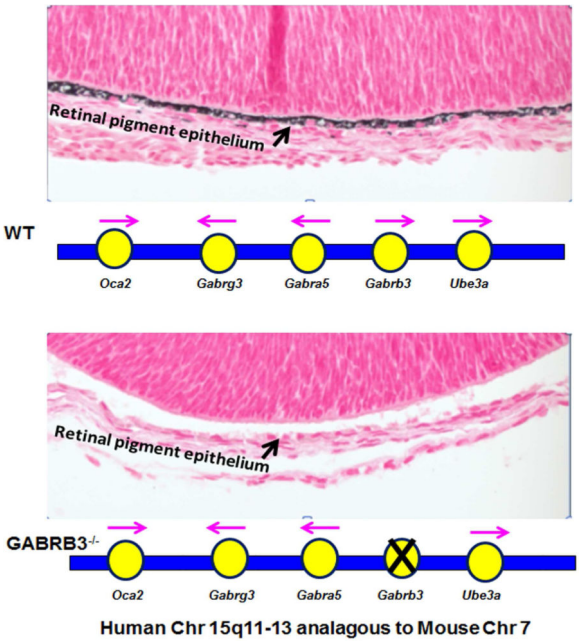

Keywords

$GABA_A$ receptors; GABRB3; OCA2; deletion; epilepsy; autism; eye; hypopigmentation

Introduction

It is well documented that reduced ocular pigmentation and other visual defects are common symptoms of Angelman syndrome (AS) and Prader-Willi syndrome (PWS) (Fryburg et al., 1991; Michieletto et al., 2011). However, the regulatory mechanisms that control gene expression in the 15q11-q13 chromosome region which includes *UBE3A*, *GABRB3*, *GABRA5*, *GABRG3* and *OCA2*, and the alterations in genes involved in AS and PWS, are complex and are not well understood (Saitoh et al., 1994). The exact function of the encoded OCA2 melanosomal transmembrane protein is unknown, but it is believed that this protein may transport molecules in and out of melanosomes where melanin is produced. The failure to transport melanin by OCA2 results in hypopigmentation. The hypopigmentation noted in AS and PWS, as well as that of oculocutaneous albinism type II, is thought to be caused simply by deletion or mutation of *OCA2*, formerly called the *P* gene (Rinchik et al., 1993), but inconsistent data exist. Hypopigmentation is present when *OCA2* is included in the deleted region with its flanking genes, but not with impairment in *OCA2* alone (Spritz et al., 1997), suggesting some unknown mechanisms underlying the phenotype of hypopigmentation in AS and PWS. Additionally, maternal deletion of *UBE3A* and

mutations in *UBE3A* alone cause AS, thus further complicating the pathogenesis of ocular pigmentation (Michieletto et al., 2011).

GABRB3 is located in the middle of the AS and PWS deletion region 15q11–13, flanked by *UBE3a*, *GABRA5*, *GABRG3* and *OCA2*. *GABRB3* is an important neurodevelopmental gene and is abundantly expressed in the early mammalian brain. Its encoded β3 subunit is important for $GABA_A$ receptor assembly, trafficking and brain development, including stem cell proliferation (Kang and Barnes, 2013; Andang et al., 2008). Genetic abnormalities in *GABRB3* have been associated with multiple brain disorders including AS, PWS (Fridman and Koiffmann, 2000; Woodage et al., 1994), childhood absence epilepsy, autism and cognitive disabilities (Tanaka et al., 2012b; Delahanty et al., 2011; DeLorey and Olsen, 1999), but the association of *GABRB3* with defects in organs other than brain has not been reported.

We report here a very robust phenotype in the mouse in which deletion of *Gabrb3* alone via disruption of its promoter and exons 1–3 caused almost complete loss of eye pigmentation. Eyes from wild-type mice in the C57BL/6J background appeared to be black while those from heterozygous $Gabrb3^{+/-}$ littermates appeared to be brown, and eyes from homozygous $Gabrb3^{-/-}$ littermates were pale yellow. With electronic microscopy, we demonstrated that melanosomes in the mutants were atrophied, and almost no mature melanosomes were detected in the retinal pigment cells in the homozygous $Gabrb3^{-/-}$ mouse eyes, while mature melanosomes were reduced in the heterozygous $Gabrb3^{-/-}$ mouse eyes. We confirmed with exome sequencing and transcriptome analysis RNA sequencing (RNA-Seq) that *Gabrb3* was the only gene that was disrupted in this model while *Oca2* gene structure was intact. Disruption of the *Gabrb3* promoter with siRNAs also down-regulated the transcripts of *Oca2* in mouse neuronal cultures. This thus suggests a mechanism in which deletion of *Gabrb3*, but not *Oca2*, could also result in the failure of melanin transport by downregulating *Oca2* transcription, thus leading to hypopigmentation. This extends the biological role of *GABRB3* beyond epilepsy and autism and provides critical insights into understanding the visual defects in AS and PWS.

Results

Deletion of Gabrb3 is associated with ocular hypopigmentation in both humans and mice

Deletion positive patients with Angelman syndrome often exhibit reduced retinal pigmentation, as illustrated by images of the eye of a patient with a Class II maternal deletion in chromosome 15q11-13 including *GABRB3* and *OCA2*, compared to his unaffected parents and sibling (Figure 1A). We made an unexpected finding in *Gabrb3* knockout mice, that heterozygous $Gabrb3^{+/-}$ mice had reduced retinal pigmentation while all the homozygous $Gabrb3^{-/-}$ mice had no visible eye pigmentation (Figure 1B) when bred in multiple different mouse genetic backgrounds including the darkly pigmented C57BL/6J.

Eyeballs from post-natal day zero (P0) wild-type $Gabrb3^{+/+}$ C57BL/6J mice appeared to be black while those from heterozygous $Gabrb3^{+/-}$ littermates appeared to be brown, and eyes from homozygous $Gabrb3^{-/-}$ littermates were pale yellow or white (Figure 1C). Consistently, the eyes in the wild-type and the heterozygous mice were black or brown while

the eyes in the homozygous pups appeared to be pink (Figure 1D). As previously described (Homanics et al., 1997), a part of the promoter and exon 1 and 3 of *Gabrb3* were replaced with the selection marker neomycin phosphotransferase (PGKneo) in the original construction of the *Gabrb3* knockout mouse model (Figure 1E).

Total protein expression of the β3 subunit encoded by *Gabrb3* in heterozygotes was reduced (0.47 ± 0.06 for het vs 1= for wt, n = 5) and no β3 subunit protein was detected in homozygotes. Total protein expression of the α5 subunit encoded by *Gabra5* in heterozygotes and homozygotes was also reduced (0.56 ± 0.08 for het and 0.16 ± 0.05 for hom vs 1= for wt, n = 5). Because mutation in *UBE3A* alone is also associated with AS, and unsilencing the dormant allele of *UBE3A* has been proposed as a therapeutic strategy for AS (Huang et al., 2012), we sought to determine the protein expression of Ube3a in the Gabrb3 knockout mice and found that Ube3a protein level was unaltered in both heterozygous and homozygous *Gabrb3* knockout mice (Figure 1F, G) (1.02 ± 0.01 for het, 0.99 ± 0.03 for hom vs 1 for wt, n = 5).

Retinal pigment epithelial (RPE) cells are the major melanin producing cells in the eye. We thus assayed the melanin in RPE cells. The proportion of homozygous mice without visible retinal pigment by both hematoxylin and eosin (H&E) staining and by visual observation was nearly 100% (n = 22 from 11 litters and 5 different dams), while about 9% of the heterozygous mice had no visible eye pigmentation (n= 35, 3/35). We then determined the melanin in the retinal pigment cell layer with Fontana Masson staining, which specifically stains melanin (Figure 1H). The average pigment intensity value in the heterozygous mice was 68% of the wild-type mice while the value in the homozygous pups was only 3% of the wild-type mice (Figure 1I). Since mutations in *UBE3A* have also been associated with AS and the *Ube3a* maternal deletion mouse model has been proposed to be the model for AS (Jiang et al., 1998) we did parallel experiments in *Ube3a* knockout mice. The full knockout *Ube3a*$^{-/-}$ mice in C57BL/6J background appeared to have normal eye pigmentation. The melanin intensity was similar between the wild-type and the *Ube3a*$^{-/-}$ mice in both H&E staining and Fontana Masson staining (Figure S1).

Melanosomes were atrophied and the mature melanosomes were reduced in the mutant Gabrb3 knockout mice

Next we used transmission electron microscopy to identify melanosomes in the RPE cells. Examination of wild-type eyes revealed all four stages of melanosome development with obvious increasing pigmentation in the latter stages. The melanosomes ranged in shapes from ovoid to circular. We found that most of the melanosomes in the RPE cells of wild-type mice were mature, while there were almost no mature melanosomes in the RPE cells in *Gabrb3*$^{-/-}$ knockout mice. In the RPE cells of heterozygous *Gabrb3*$^{+/-}$ mice, the intensity of melanosomes and the number of mature melanosomes were reduced (103 ± 12, n = 25 for wt 71 ± 7, n = 55 for het, 18 ± 3, n = 40 for hom). Melanosomes of all different stages were observed in wild-type and heterozygous mice. However, there were more III-IV stage melanosomes (83 ± 4, n = 7 for wt 61 ± 7, n = 8 for het, 0 ± 0, n=8 for hom) and fewer I-II stage melanosomes (17 ± 5, n = 7 for wt 39 ± 7, n = 8 for het, 100 ± 0.10, n = 8 for hom) in the wild-type than in heterozygous and homozygous mice (Figure 2 A, B, C). There were no

melanosomes at III-IV stages detected in the homozygous eye. As shown in the enlarged images, samples from both wild-type and heterozygous mice had melanosomes at different stages (Figure S2). Samples from homozygous mice, however, had only stage I immature melanosomes, and some of these melanosomes exhibited abnormal morphology. Contrary to both wild-type and heterozygous eyes, the homozygous eyes were devoid of the darker electron dense mature melanocytes (Figure S2). The ultra-structure was poorly maintained showing many open spaces not evident in wild-type eyes. The loss of tissue integrity was unlikely due to experimental procedures because the finding was consistent from multiple mice (Figure S2). It is unknown if the loss of *Gabrb3* or alteration of other genes due to the disruption of *Gabrb3* would affect cytoskeleton or microtubule networks which could lead to a compromise in tissue integrity. Nevertheless, this suggests that some unknown mechanisms may underlie the defects in tissue integrity especially in the homozygous mice, but this issue needs further investigation.

Melanosomes from the Gabrb3 knockout mice were more diffusely distributed and less clustered

The distribution of melanosomes in the RPE cells from wild-type mice were clustered and concentrated apically, while the melanosomes from the heterozygous mice were more diffusely distributed and less clustered. The melanosomes in RPE cells from homozygous mice were distributed more diffusely than in the wild-type and RPE cells from heterozygous mice (Figure 2D). We then measured the span of the melanosome distribution which is the width of the layer of melanosome for each genotype and found that the span was longest in homozygous mice (0.54 ± 0.02 μm, n = 4 for wt 0.78 ± 0.07 μm, n = 4 for het, 1.2 ± 0.14 μm, n = 4 for hom) (Figure 2E). The melanosomes in the wild-type were localized to a single layer within the eye. In the heterozygous eyes, the overall ultra-structural organization was less precise than wild-type and the melanosomes were not confined to a single layer within the eye. In the homozygous eye, the early stage immature melanosomes were not confined to a distinct layer within the eye, but rather extended into the deeper layers. This suggests abnormalities in cellular architecture but needs further elucidation. In the mutant mice, there was a reduction in the total number of melanosomes, including the stage I-IV melanosomes) (29.57 ± 1.6, n = 7 for wt 19.9 ± 1.56, n = 10 for het, 1.71 ± 0.36, n = 7 for hom) (Figure 2 F, G). It is interesting that the distribution pattern of melanosomes is similar between the wild-type and the heterozygous but was very different for the homozygous mice. It is likely that there are some unknown compensatory cellular mechanisms that could attenuate the phenotype in the heterozygous but not in the homozygous, mice. A similar phenomenon has been noticed in the phenotype for another $GABA_A$ receptor subunit gene *GABRG2*. In *Gabrg2* knockout mice, the homozygous knockout was lethal while the heterozygous knockout only had mild absence epilepsy and anxiety but a normal survival (Warner et al., 2016; Xia et al., 2016). The lack of pigmentation in the $Gabrb3^{-/-}$ mice is likely to be due to the defects in melanin transport and melanosome maturation instead of melanin synthesis because there was no change with tyrosine hydroxylase staining (Figure S3).

Only Gabrb3 transcripts were absent in Gabrb3 knockout mice but multiple genes in eye morphogenesis and amine binding were upregulated while genes in neuroactive ligand

receptors, calcium signaling pathway and steroid synthesis were downregulated in Gabrb3 knockout mice

GABRB3 is flanked by *UBE3A*, *GABRA5*, *GABRG3* and *OCA2* in both human and mouse (Figure 3A). We then performed high-throughput RNA-Seq for the total brain tissues to determine gene expression at the transcriptional level (Figure 3B). Only *Gabrb3* was substantially down-regulated in the hom *Gabrb3*$^{-/-}$ mouse (−11.19 fold) while other flanking genes had minimal downregulation compared with the wild-type (−0.31 for *Oca2*, −0.08 for *Gabrg3*, −0.13 for *Gabra5* and −0.24 for *Ube3a*) (Figure 3B). As indicated in the heat map and the gene ontology results (Figure 3C, Figure S3 and Table S1), the relative expression of many genes was altered, especially those involved in eye morphogenesis, amine binding, neuroactive ligand receptor interaction, calcium signaling and neurotransmitter receptor activity and steroid biosynthesis. However, the expression of genes related to pigment synthesis were unchanged, as were $GABA_A$ receptor genes in other chromosomes. Unaltered expression of pigment synthesis related genes further validates that the reduced pigmentation is due to defects in melanin transport and melanosome maturation instead of melanin synthesis. However, the RNA-Seq data suggest that the *Gabrb3* deletion has far-reaching impact on neurodevelopment and the significance of these extensive gene alterations needs to be further explored (Table S1).

Silencing Gabrb3 against its promoter but not the middle coding region down-regulated Oca2 transcripts

What is the genetic basis for a disruption of *Gabrb3* causing hypopigmentation? We hypothesized that it was due to the disruption of *Gabrb3* that indirectly down-regulated *Oca2* but not the impairment of β3 subunit itself. We then designed siRNAs targeting the promoter region and coding region of *Gabrb3* to determine the effect on transcription of *Gabrb3* and *Oca2* in mouse neuronal culture (Figure S3, Figure 3D). We found that disruption of either the promoter region or of exon 4 by siRNAs down-regulated the expression of *Gabrb3* (0.11 ± 0.07 for promoter, 0.24 ± 0.18 for exon 4 vs 0.97 ± 0.15 for scramble, n = 4 cultures) (Figure 3E). However, only disruption of the promoter region, but not the coding region, of exon 4 (Figure 3F) specifically downregulated the transcripts of *Oca2* (0.25 ± 0.16 for promoter, 0.79 ± 0.23 for exon 4 vs 1.06 ± 0.09 for scramble, n = 4 cultures).

We then determined if an increase of β3 subunit protein and $GABA_A$ receptor function would up-regulate *Oca2* expression. We thus over-expressed human GABRB3 cDNA with an HA tag, which prevents it from being detected by the probes against mouse *Gabrb3* transcripts because of the insertion of HA tag in the probed region. We demonstrated that increasing the β3 subunit protein by over-expression of the $GABRB3^{HA}$ subunit cDNAs in neurons did not upregulate the expression of *Oca2* (0.68 ± 0.18 for het and 0.27 ± 0.06 for hom without $β3^{HA}$ subunit protein vs 0.58 ± 0.12 for het and 0.24 ± 0.08 for hom with $β3^{HA}$ subunit protein) or *Gabrb3* transcripts (0.46 ± 0.12 for het 0.04 ± 0.01 for hom without $β3^{HA}$ subunit protein vs 0.49 ± 0.08 for het 0.05 ± 0.01 for hom with $β3^{HA}$ subunit protein) in the neuronal cultures (Figure 3G). This thus suggests that the downregulation of *Oca2* in *Gabrb3* knockout mice was not due to loss of $β3^{HA}$ subunit protein and the function of GABRB3 subunit containing receptor per se. It is instead likely that some unknown transcriptional mechanisms involving the *Gabrb3* promoter region which modulates the expression of the

downstream gene like *Oca2*. It has been reported that *GABRB3* has a strong promoter (Kirkness and Fraser, 1993). It is possible that the *GABARB3* promoter or its associated binding proteins may regulate the transcription of adjacent genes. However, this requires further elucidation.

Though Gabrb3 is the only deleted gene, transcripts of the downstream genes such as Gabra5, Gabrg3 and Oca2 were downregulated

Because the chromosome 15q11-13 region is unstable, and genomic abnormalities like deletion or duplication are frequently identified in this region, we performed mouse whole exome sequencing to make sure that this mouse line had no mutations or other genetic abnormalities other than the *Gabrb3* deletion. Our data verified that only the first two exons and part of exon 3 of *Gabrb3* were absent, while the downstream exons of *Gabrb3* and those of the flanking genes, including the 11 exons of *Oca2*, were intact (Figure 4 A, B). This is consistent with the original construction of the *Gabrb3* knockout mouse, in which the 2.8 kb of the *Gabrb3* promoter and exon 1–3 regions were replaced (Homanics et al., 1997). This thus indicated that the *Oca2* gene itself was unaltered in the *Gabrb3* knockout mouse and confirms that only the *Gabrb3* gene region was interrupted in this mouse model.

What is the basis for hypopigmentation in the *Gabrb3* knockout mice if the *Oca2* gene is intact? RNA-Seq data indicated a minimal down-regulation of the transcripts of adjacent genes, although the Gabrb3 transcripts were absent. We then quantified transcripts of five *Gabrb3* flanking genes including *Ube3a*, *Gabra5*, *Gabrg3* and *Oca2* via qRT-PCR in both brain and eye tissues. Expression of *Oca2* mRNA was reduced in the mutant *Gabrb3* mouse whole brain tissue, cerebellar tissue and eye samples (Figure 4C, D, E). The relative expression profile of *Oca2* in eye tissue (Figure 4E) (0.46 ± 0.07 for het, 0.12 ± 0.05 for hom vs 1.0 for wt, n = 3 pairs of mice) was similar to *Gabrb3* (0.53 ± 0.015 for het, 0.0 for hom vs 1.0 for wt, n = 3 pairs of mice for eye) and forebrain (Figure 4F) from each genotype. Although *Oca2* mRNA abundance is low in forebrain, it is evident that *Oca2* transcripts were reduced in the mutant *Gabrb3* knockout compared with the wild-type mouse (Figure 4 F). *Gabra5* and *Gabrg3* mRNA expression was also reduced (0.65 ± 0.07 for het, 0.12 ± 0.05 for hom for *Gabra5*, and 0.61 ± 0.15 for het and 0.25 ± 0.16 for hom for *Gabrg3* vs 1.0 for wt, n = 3 pairs of mice), but expression of *Ube3a* was not reduced (Figure 4 F).

We also determined the expression levels of $GABA_A$ receptor genes that are not located in chromosome 15q11-13 but have close interaction with *Gabrb3* during receptor assembly and biogenesis. These include *Gabra1* and *Gabra3* as well as a few essential genes for neuronal and eye development, including *Mitf, Pax6*, *Wnt3A*, to exclude any defect of these essential transcriptional factors that could explain alterations in RPE cell differentiation(Martinez-Morales et al., 2004). The data demonstrated that *Gabra1* (0.98 ± 0.12 for het, 1.04 ± 0.11 for hom vs 1 for wt, n = 3 pairs of mice) and *Gabra3* (1.08 ± 0.17 for het, 0.99 ± 0.11 for hom vs 1 for wt, n = 3 pairs of mice) gene expression in the *Gabrb3* knockout mice was unaltered. The mRNA abundance of *Mitf* (1.14 ± 0.15 for het, 1.05 ± 7 for hom vs 1 for wt, n = 3 pairs of mice), *Pax6* (1.21 ± 0.19 for het, 1.06 ± 0.14 for hom vs 1 for wt, n = 3 pairs of mice) and *Wnt3a* (1.22 ± 0.21 for het, 1.30 ± 0.20 for hom vs 1.00 for wt, n = 3 pairs of mice) was also unaltered (Figure 4G), suggesting that the hypopigmentation found in

Gabrb3 knockout mice was likely due to the down-regulation of *Oca2* transcripts. It is not clear why only minimal downregulation of *Oca2* and other adjacent genes was observed with RNA-Seq. One possible explanation is that total RNAs for the RNA-Seq assay were from whole brain lysates while the RNAs for qRT-PCR data were acquired from more specific brain regions such as cerebellum, forebrain or eyes.

Discussion

We first identified that a deletion of *Gabrb3* alone unexpectedly caused almost complete loss of eye pigment in mice. It has been commonly observed that reduced ocular pigmentation exists in AS and PWS (King et al., 1993). It has long been thought to be caused by *OCA2* deletion and not related to *GABRB3* deletion. However, there is a report that ocular hypopigmentation in the PWS correlates with P gene deletion but not with haplotype of the hemizygous P allele (Spritz et al., 1997), suggesting genes other than *Oca2* in the region may be involved in contributing to hypopigmentation. It is well established that *GABRB3* impairment is associated with epilepsy, autism and other neurodevelopmental disorders (Tanaka et al., 2012b; Delahanty et al., 2011). Deletion in chromosome 15q11-13, a region, which includes the *GABRB3* gene, is the major cause of AS and PWS (Williams et al., 1995). In addition to seizures, AS and PWS often exhibit clinical features that are characteristic of tyrosine-positive (Type II) OCA albinism (Rinchik et al., 1993). Reduced retinal pigmentation in AS and PWS is associated with multiple visual defects including reduced visual acuity, nystagmus and strabismus (Fryburg et al., 1991). It had previously been concluded that this reduced pigmentation was caused by deletion of *OCA2* (also known as *P*) (Rinchik et al., 1993) because the region of deletion in AS and PWS often includes *OCA2*. Our findings indicate that deletion of *GABRB3* alone could result in a complex eye phenotype in addition to the epilepsy or autism phenotypes resulting from the loss of function of β3 subunit itself, by affecting the expression of adjacent genes, including *OCA2*.

The downregulation of genes adjacent to *Gabrb3* was unexpected in *Gabrb3* knockout mice, although a previous study found that mutations in a regulatory element located within the *Herc2* gene inhibited *Oca2* gene expression, giving rise to blue and brown eye colors (Eiberg et al., 2008). Here we have unequivocally demonstrated in *Gabrb3* knockout mice, that *Oca2* mRNA was substantially reduced in both the eyeball and brain tissues, suggesting that an unknown mechanism is downregulating the expression of adjacent genes flanking *Gabrb3* at the transcriptional level because *Oca2* gene structure was unaltered (Figure 4A and B). This may suggest a shared promoter or some unknown transcriptional mechanisms involving the *GABRB3* exon 1–3 region that is critical for *Oca2* gene expression. It has also been previously reported that an intron in *HERC2* contains the promoter region for *Oca2*, suggesting complex transcriptional regulation of *Oca2* by its adjacent genes (White and Rabago-Smith, 2011). The *GABRB3* promoter region is critical for transcriptional factor binding (Tanaka et al., 2012a) and splicing as previously demonstrated (Kirkness and Fraser, 1993). It is possible that the *GABRB3* promoter may regulate transcription of adjacent genes via unknown mechanisms.

High throughput RNA sequencing of the *Gabrb3*$^{-/-}$ knockout mouse demonstrated that only *Gabrb3* transcripts were absent, while *Oca2* transcripts have very low baseline expression in mouse brain. Given the fact that *GABRB3* is expressed in both embryonic stem (ES) cells and neural crest stem (NCS) cells (Andang et al., 2008), which give rise to a diverse cell lineage including melanocytes, it is possible that *GABRB3* deletion would cause diverse abnormalities, including cell differentiation from conception on in the embryo. This is also implicated by the previous finding that *Gabrb3* deletion causes cleft palate (Homanics et al., 1997). It has been demonstrated that autocrine/paracrine GABA signaling by means of $GABA_A$ receptors negatively control ES cell and peripheral NCS cell proliferation (Andang et al., 2008). Additionally, the promoter region of *Gabrb3* binds multiple transcriptional factors involved in stem cell differentiation. Future studies focusing on stem cell differentiation and cell lineage tracing in combination with *in vivo Gabrb3* knockout will further elucidate the critical role of *GABRB3* in brain and eye development and related neurodevelopmental disorders.

In conclusion, this study has unequivocally demonstrated in the mouse that disruption of *Gabrb3* alone in the promoter region causes a downregulation of *Oca2. This* downregulation of *Oca2* by interruption of *Gabrb3* results in failure of melanin transport and arrested melanosome maturation, leading to ocular hypopigmentation. However, based on this study, the role of *GABRB3* in ocular hypopigmentation is unlikely via the function of β3 subunit in $GABA_A$ receptors but via regulation of the expression of *Oca2*, which is the gene that is directly involved in melanin transport. Considering the conventional role of *GABRB3* in epilepsy and neurodevelopmental disorders like autism, this finding extends our understanding of *GABRB3* beyond those neuropsychiatric disorders.

Methods and Materials

Human eye image

The human eye images from a family of an AS patient in Figure 1A were provided by Dr. Terry Jo Bichell.

Mice

The *Gabrb3* knockout mouse line has been previously generated (DeLorey et al., 1998) and was obtained from Jackson Laboratory. Genotyping was performed following the instructions from Jackson Laboratory. Heterozygous x heterozygous breeding was carried out in C57BL/6J/S129 mixed background and C57BL/6J background. The eyeball and total brain lysates from an *Ube3a* knockout mouse line in C57BL/6J originally derived by Jiang (Jiang et al., 1998) were kindly provided by Dr. Andre Lagrange's lab in the Department of Neurology, Vanderbilt University Medical Center. Only P0 day old pups were included.

Eye sample preparations and immunohistochemistry

Eye samples were paraffin embedded in a desired orientation and sectioned at 5 μm. Sectioned brain slices were mounted on Superfrost Plus slides for immunohistochemical studies. The H&E, Fontana Masson staining, and immunohistochemistry were performed

with standard procedures in the Vanderbilt Translational Pathology Shared Resource Core (Kang et al., 2015).

Total RNA extraction and qRT-PCR

Total RNA from both eyes and whole brain tissue of P0 pups were extracted with Trizol/chloroform. For qRT-PCR, the cDNAs of all samples were prepared with a Reverse Transcription kit (Invitrogen). We performed qRT-PCR using an Applied Biosystems 7900 with the TaqMan Universal Master Mix and with 6-carboxyfluorescein (FAM)-labeled probes (Applied Biosystems) for each specific gene and a VIC-labeled probe (Applied Biosystems) for the endogenous control, β-actin (4352341E). The specific gene expression was normalized to mouse β-actin (Applied Biosystems) (Kang et al., 2009b).

Neuronal cultures, transfections and siRNAs

Neuronal cultures and delivery of siRNAs were modified from our previous study (Kang et al., 2009a). Mice were genotyped immediately after they were born. Mouse cortice were dissected from the brains of postnatal day 0 (P0) old C57BL/6J pups. Brain tissues from pups with the same genotype were combined for cultures. Human $GABRB3^{HA}$ cDNAs were transfected into neurons by calcium precipitation method as previously described (Kang et al., 2010). SiRNAs were prepared according to the manufacturer's instructions (Thermo Fisher Scientific), and siRNAs (50 nM) were transfected with Oligofectamine or Lipofectamine (Invitrogen) to cells on the $4–5^{th}$ day in cultures and were harvested 7–8 days later which was around 12 days old in culture.

Statistical analysis

Protein integrated density values (IDVs) were quantified by using the Quantity One or Odyssey fluorescence imaging system (Li-Cor). Images were quantified by ImageJ software. Data were expressed as mean ± S.E.M values and analyzed with Graphpad Prism 5.0 software. Statistical significance of immunoblot, cell imaging and qRT-PCR data was determined by a Student's unpaired t test or, if appropriate, single value t test. All analyses used an alpha level of 0.05 to determine statistical significance.

Supplementary Material

Refer to Web version on PubMed Central for supplementary material.

Acknowledgments

This research was supported by research grants from Citizen United for Research in Epilepsy (CURE), Dravet syndrome foundation (DSF), IDEAleague (Dravet organization) and Vanderbilt Clinical and Translation Science Award (CTSA), NIH R01NS 082635 to KJQ. TB was supported by training program T32ES007028.

Reference List

Andang M, Hjerling-Leffler J, Moliner A, Lundgren TK, Castelo-Branco G, Nanou E, Pozas E, Bryja V, Halliez S, Nishimaru H, Wilbertz J, Arenas E, Koltzenburg M, Charnay P, El MA, Ibanez CF, Ernfors P. Histone H2AX-dependent GABA(A) receptor regulation of stem cell proliferation. Nature. 2008; 451:460–464. [PubMed: 18185516]

Delahanty RJ, Kang JQ, Brune CW, Kistner EO, Courchesne E, Cox NJ, Cook EH Jr, Macdonald RL, Sutcliffe JS. Maternal transmission of a rare GABRB3 signal peptide variant is associated with autism. Mol. Psychiatry. 2011; 16:86–96. [PubMed: 19935738]

DeLorey TM, Handforth A, Anagnostaras SG, Homanics GE, Minassian BA, Asatourian A, Fanselow MS, Delgado-Escueta A, Ellison GD, Olsen RW. Mice lacking the beta3 subunit of the GABAA receptor have the epilepsy phenotype and many of the behavioral characteristics of Angelman syndrome. J. Neurosci. 1998; 18:8505–8514. [PubMed: 9763493]

DeLorey TM, Olsen RW. GABA and epileptogenesis: comparing gabrb3 gene-deficient mice with Angelman syndrome in man. Epilepsy Res. 1999; 36:123–132. [PubMed: 10515160]

Eiberg H, Troelsen J, Nielsen M, Mikkelsen A, Mengel-From J, Kjaer KW, Hansen L. Blue eye color in humans may be caused by a perfectly associated founder mutation in a regulatory element located within the HERC2 gene inhibiting OCA2 expression. Hum. Genet. 2008; 123:177–187. [PubMed: 18172690]

Fridman C, Koiffmann CP. Origin of uniparental disomy 15 in patients with Prader-Willi or Angelman syndrome. Am. J. Med. Genet. 2000; 94:249–253. [PubMed: 10995513]

Fryburg JS, Breg WR, Lindgren V. Diagnosis of Angelman syndrome in infants. Am. J. Med. Genet. 1991; 38:58–64. [PubMed: 2012134]

Homanics GE, DeLorey TM, Firestone LL, Quinlan JJ, Handforth A, Harrison NL, Krasowski MD, Rick CE, Korpi ER, Makela R, Brilliant MH, Hagiwara N, Ferguson C, Snyder K, Olsen RW. Mice devoid of gamma-aminobutyrate type A receptor beta3 subunit have epilepsy, cleft palate, and hypersensitive behavior. Proc. Natl. Acad. Sci. U. S. A. 1997; 94:4143–4148. [PubMed: 9108119]

Huang HS, Allen JA, Mabb AM, King IF, Miriyala J, Taylor-Blake B, Sciaky N, Dutton JW Jr, Lee HM, Chen X, Jin J, Bridges AS, Zylka MJ, Roth BL, Philpot BD. Topoisomerase inhibitors unsilence the dormant allele of Ube3a in neurons. Nature. 2012; 481:185–189.

Jiang YH, Armstrong D, Albrecht U, Atkins CM, Noebels JL, Eichele G, Sweatt JD, Beaudet AL. Mutation of the Angelman ubiquitin ligase in mice causes increased cytoplasmic p53 and deficits of contextual learning and long-term potentiation. Neuron. 1998; 21:799–811. [PubMed: 9808466]

Kang JQ, Barnes G. A common susceptibility factor of both autism and epilepsy: functional deficiency of GABA A receptors. J. Autism Dev. Disord. 2013; 43:68–79. [PubMed: 22555366]

Kang JQ, Shen W, Macdonald RL. Two molecular pathways (NMD and ERAD) contribute to a genetic epilepsy associated with the GABA(A) receptor GABRA1 PTC mutation, 975delC, S326fs328X. J. Neurosci. 2009b; 29:2833–2844. [PubMed: 19261879]

Kang JQ, Shen W, Zhou C, Xu D, Macdonald RL. The human epilepsy mutation GABRG2(Q390X) causes chronic subunit accumulation and neurodegeneration. Nat. Neurosci. 2015; 18:988–996. [PubMed: 26005849]

King RA, Wiesner GL, Townsend D, White JG. Hypopigmentation in Angelman syndrome. Am. J. Med. Genet. 1993; 46:40–44. [PubMed: 8494033]

Kirkness EF, Fraser CM. A strong promoter element is located between alternative exons of a gene encoding the human gamma-aminobutyric acid-type A receptor beta 3 subunit (GABRB3). J. Biol. Chem. 1993; 268:4420–4428. [PubMed: 8382702]

Martinez-Morales JR, Rodrigo I, Bovolenta P. Eye development: a view from the retina pigmented epithelium. Bioessays. 2004; 26:766–777. [PubMed: 15221858]

Michieletto P, Bonanni P, Pensiero S. Ophthalmic findings in Angelman syndrome. J. AAPOS. 2011; 15:158–161. [PubMed: 21596294]

Rinchik EM, Bultman SJ, Horsthemke B, Lee ST, Strunk KM, Spritz RA, Avidano KM, Jong MT, Nicholls RD. A gene for the mouse pink-eyed dilution locus and for human type II oculocutaneous albinism. Nature. 1993; 361:72–76. [PubMed: 8421497]

Saitoh S, Harada N, Jinno Y, Hashimoto K, Imaizumi K, Kuroki Y, Fukushima Y, Sugimoto T, Renedo M, Wagstaff J. Molecular and clinical study of 61 Angelman syndrome patients. Am. J. Med. Genet. 1994; 52:158–163. [PubMed: 7802001]

Spritz RA, Bailin T, Nicholls RD, Lee ST, Park SK, Mascari MJ, Butler MG. Hypopigmentation in the Prader-Willi syndrome correlates with P gene deletion but not with haplotype of the hemizygous P allele. Am. J. Med. Genet. 1997; 71:57–62. [PubMed: 9215770]

Tanaka M, Bailey JN, Bai D, Ishikawa-Brush Y, Delgado-Escueta AV, Olsen RW. Effects on promoter activity of common SNPs in 5' region of GABRB3 exon 1A. Epilepsia. 2012a; 53:1450–1456. [PubMed: 22765836]

Tanaka M, DeLorey TM, Delgado-Escueta A, Olsen RW. GABRB3, Epilepsy, and Neurodevelopment. 2012b

Warner TA, Shen W, Huang X, Liu Z, Macdonald RL, Kang JQ. DIfferential molecular and behavioral alterations in mouse models of GABRG2 haploinsufficiency versus dominant negative mutations associated with human epilepsy. Hum. Mol. Genet. 2016

White D, Rabago-Smith M. Genotype-phenotype associations and human eye color. J. Hum. Genet. 2011; 56:5–7. [PubMed: 20944644]

Williams CA, Angelman H, Clayton-Smith J, Driscoll DJ, Hendrickson JE, Knoll JH, Magenis RE, Schinzel A, Wagstaff J, Whidden EM. Angelman syndrome: consensus for diagnostic criteria. Angelman Syndrome Foundation. Am. J. Med. Genet. 1995; 56:237–238. [PubMed: 7625452]

Woodage T, Deng ZM, Prasad M, Smart R, Lindeman R, Christian SL, Ledbetter DH, Robson L, Smith A, Trent RJ. A variety of genetic mechanisms are associated with the Prader-Willi syndrome. Am. J. Med. Genet. 1994; 54:219–226. [PubMed: 7810579]

Xia G, Pourali P, Warner TA, Zhang CQ, Macdonald L, Kang JQ. Altered GABAA receptor expression in brainstem nuclei and SUDEP in Gabrg2(+/Q390X) mice associated with epileptic encephalopathy. Epilepsy Res. 2016; 123:50–54. [PubMed: 27131289]

In Brief

Hypopigmentation in Angelman syndrome is thought to stem from deletion of the pigment gene *OCA2*. Delahanty *et al* now find that disruption of *Gabrb3* alone causes profound loss of retinal pigmentation via downregulation of *Oca2* transcription. This suggests unique complexities in gene regulation in the 15q11-13 imprinted region.

Highlights

Gabrb3 and *Oca2* are located within the Angelman-Prader-Will imprinted region.

Oca2 is associated with ocular hypopigmentation while *Gabrb3* encodes a $GABA_AR$ subunit.

Mice with *Gabrb3* disruption have reduced eye pigmentation due to melanosome atrophy.

Disruption of the *Gabrb3* promoter region alone downregulates transcription of *Oca2*.

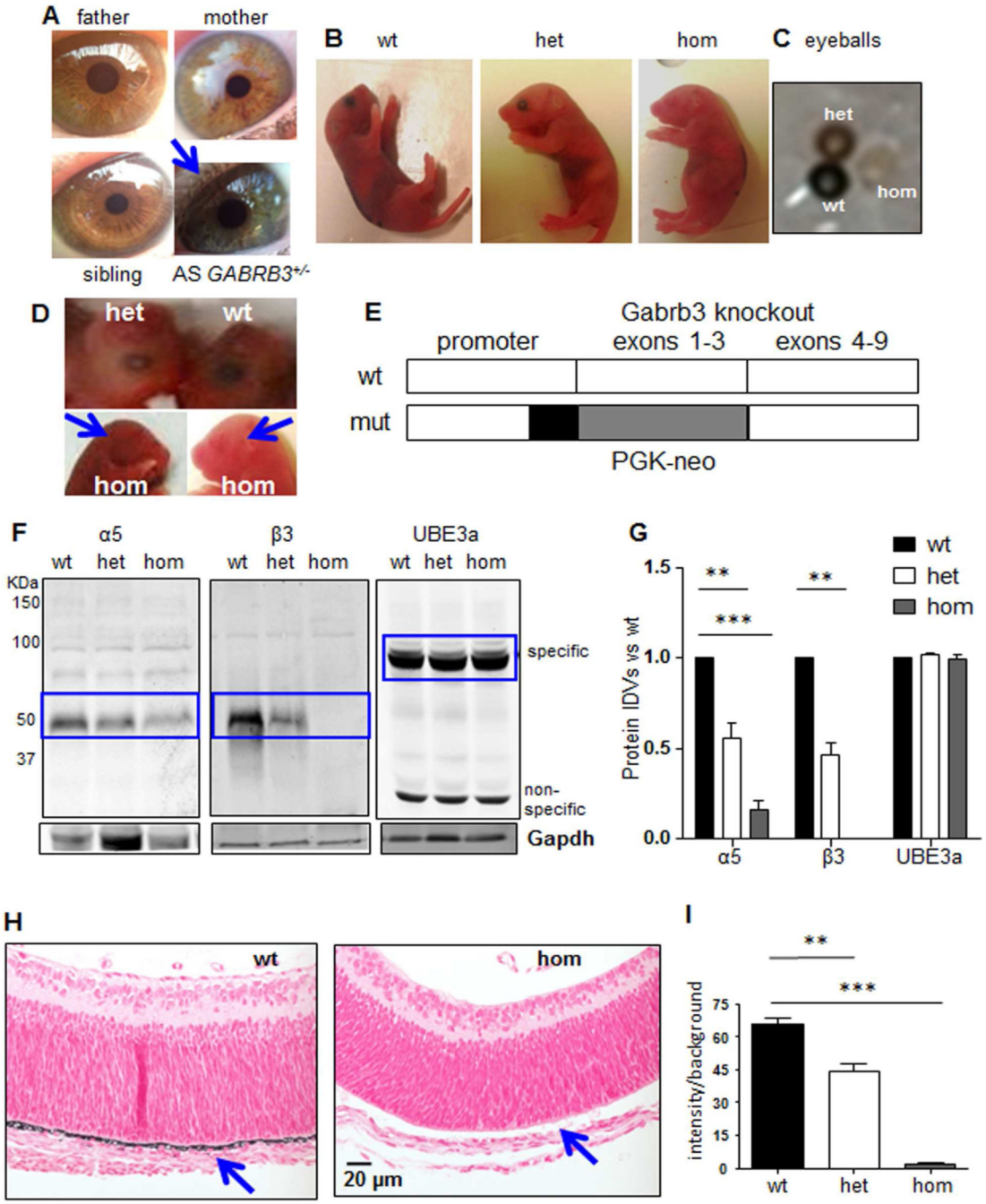

Figure 1. Deletion of Gabrb3 including the promoter region is associated with ocular hypopigmentation in both humans and mice

(A). Representative eye images of the normal parents and sibling of a child with Angelman syndrome (AS) caused by a Class II maternal deletion in chromosome 15 containing the *GABRB3 and OCA2* genes. The eye color of the AS child as indicated by blue arrow was lighter than that of both parents and the sibling. (B). Images of wild-type (wt) *Gabrb3*$^{+/+}$, heterozygous (het) *Gabrb3*$^{+/-}$, and homozygous (hom) *Gabrb3*$^{-/-}$ knockout (KO) mice at post-natal day 0 (P0). (C). Images of dissected eyeballs from P0 wt, het and hom *Gabrb3* KO mice. (D). A close up image of the P0 wt, het and hom *Gabrb3* KO mouse eyes. There was

no obvious pigment in the hom eyes as indicated by blue arrows. (E). A schematic illustration of GABRB3 knockout construct, ie. a part of the *Gabrb3* promoter and exon 1–3 were replaced by neomycin phosphotransferase (PGKneo) in *Gabrb3* KO mice. (F). Representative blots for protein expression of α5 subunit (~50 kDa), β3 subunit (~50 kDa) and UBE3a (~90 kDa) in cerebellar lysates of P0 wt, het and hom *Gabrb3* KO mice. The specific band in each gel was highlighted by blue box. Gapdh (~37 kDa) used as loading control. (G). Quantification of relative α5, β3 and UBE3a protein integrated density values (IDVs) in *Gabrb3* KO mice (n = 4). (H). Fontana Masson (FM) staining indicating that P0 hom *Gabrb3* KO mice had no visible melanin in retinal pigment epithelial (RPE) cells, a layer which was distinct in wt, as indicated by the blue arrow. (I). Histogram showing P0 het and hom *Gabrb3* KO mice had reduced melanin intensity in retinal pigment epithelial cells from FM staining compared to P0 wt littermates (n = 6).

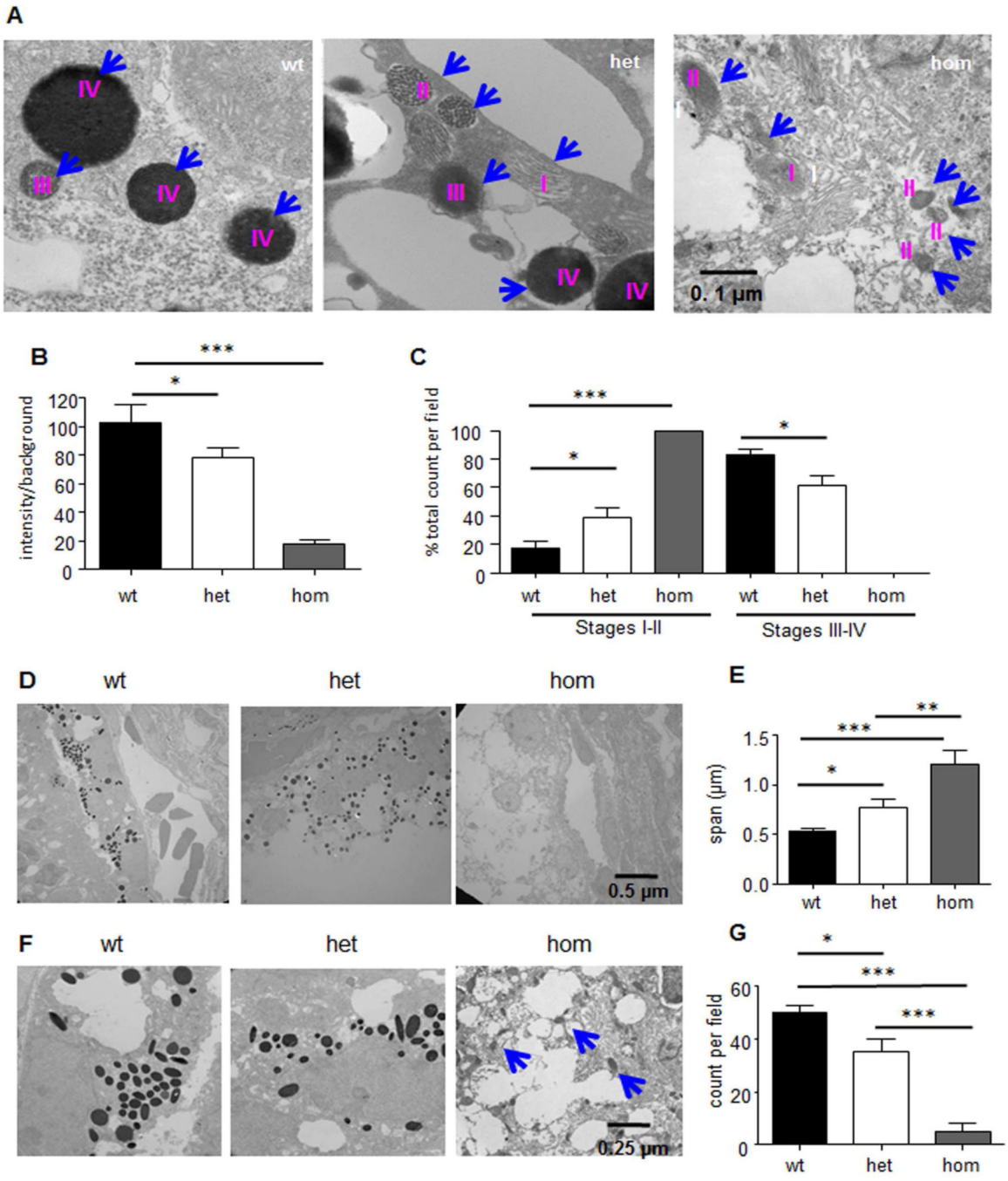

Figure 2. Melanosomes in Gabrb3 knockout mice were less mature, reduced in total numbers and more diffusely distributed

(A). Representative images from transmission electron microscopy (TEM) of retinal pigment epithelial (RPE) cells showing melanosomes in P0 wild-type (wt) *Gabrb3*$^{+/+}$, heterozygous (het) *Gabrb3*$^{+/-}$, and homozygous (hom) *Gabrb3*$^{-/-}$ knockout (KO) mice. Blue arrows point to the location of melanosomes, while pink roman numerals indicate the stage of each melanosome. (B). Quantification of TEM image intensity (over background) normalized to wt. (C). Percent of total number of melanosomes per field at different stages by genotype. (D). Representative TEM images of RPE cells (2700X) from P0 wt, het and hom *Gabrb3*

KO eyeballs. (E). Quantification of span of melanosomes in μm by genotype. (F). Representative TEM images of RPE cells (6500X) from P0 wt, het and hom *Gabrb3* KO eyeballs (indicated by the blue arrows for hom *Gabrb3* sample). (G). Quantification of number of melanosomes per field from TEM images of RPE cells. The P0 het mice had reduced mature melanosomes, compared to wt, while those from hom mice had minimal to no mature melanosomes. In B, C, E and G, *$p < 0.05$; ** $p < 0.01$; *** $p < 0.001$, $n = 4$ mice for each genotype.

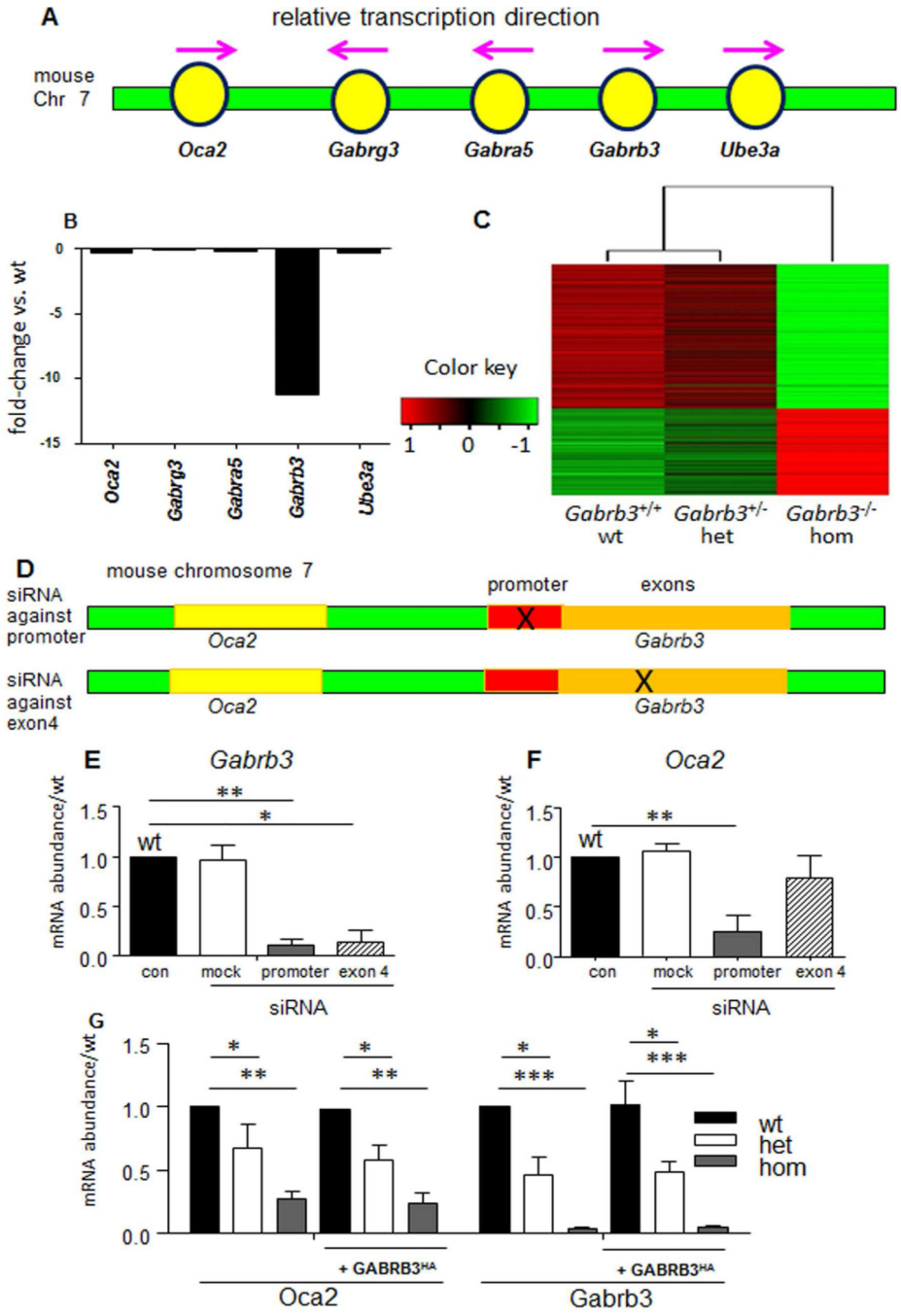

Figure 3. Only Gabrb3 transcripts were absent in RNA-Seq but disruption of Gabrb3 promotor by siRNAs down-regulated Oca2 gene expression in mouse neurons

(A) Schematic illustration of *Gabrb3* and flanking genes in mouse chromosome 7. Magenta arrows indicate the transcription direction of each gene. (B). Fold-change of transcripts from genes flanking *Gabrb3* from RNA-sequencing (RNA-Seq) in P0 homozygous (hom) $Gabrb3^{-/-}$ knockout (KO) mice when normalized to wild-type (wt) $Gabrb3^{+/+}$ values. (C). The heatmap demonstrates that expression of many genes was altered in the P0 hom *Gabrb3* mice compared with the wt and heterozygous (het) mice as reflected by color key. (D). Schematic illustration of *Gabrb3* and flanking *Oca2* in mouse chromosome 7. (E, F). The

relative mRNA abundance of *Gabrb3* (E) or *Oca2* (F) in two week old mouse cortical neurons treated with or without siRNAs for 4 days measured by qRT-PCR. Con indicates untreated control neurons, mock indicates neurons treated with scrambled siRNAs. Promoter signifies neurons treated with siRNAs targeting the *Gabrb3* promoter region while exon 4 signifies those targeting *Gabrb3* exon 4. (G). Neuronal cultures were transfected with HA tagged human GABRB3 subunit ($GABRB3^{HA}$) cDNAs for 7–8 days. Relative abundance of *Oca2* and *Gabrb3* transcripts in neurons from *Gabrb3* knockout pups of each genotype with or without over-expression of $GABRB3^{HA}$ cDNA. In E, F and G, *$p < 0.05$; ** $p < 0.01$; *** $p < 0.001$ vs wt.

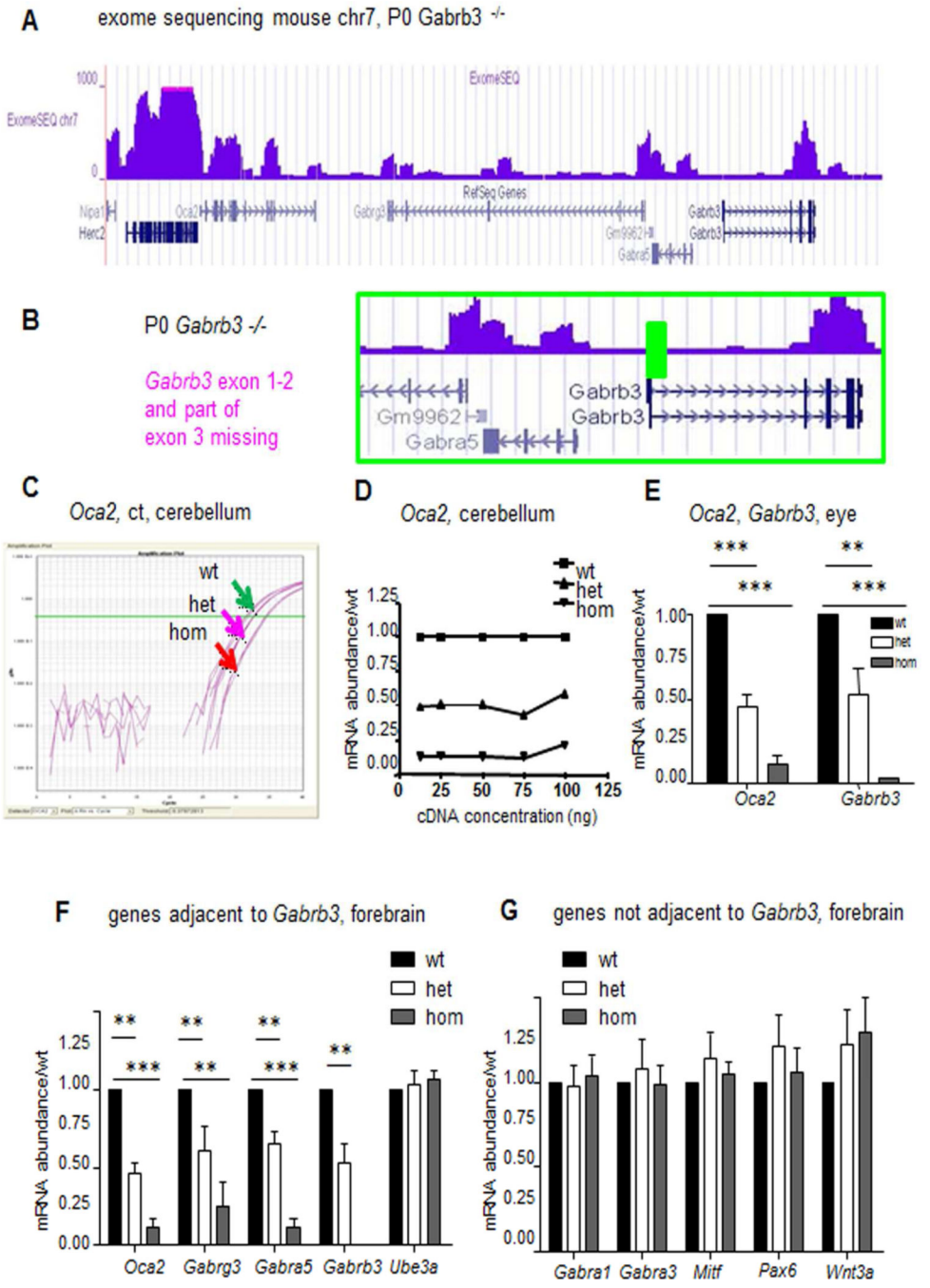

Figure 4. Deletion of Gabrb3 including the promoter region downregulated expression of Oca2in the eye as well as in the brain

(A). Whole exome sequencing of eyeball from P0 homozygous (hom) *Gabrb3*$^{-/-}$ KO mouse determined that only the early exons 1–3 in *Gabrb3* were absent while the adjacent genes were intact. (B). Enlarged view of *Gabrb3* and adjacent regions by exome sequencing. The green block indicates the deleted region of *Gabrb3 in Gabrb3*$^{-/-}$ mice. (C–E). Total RNA was extracted from the cerebella, eyeballs or the forebrains of the newborn wild-type (wt), heterozygous (het) and homozygous (hom) *Gabrb3*$^{-/-}$ littermates. The total RNAs were transcribed to cDNA and quantified by qRT-PCR. The plot demonstrated the Delta CT

values of *Oca2* expression in wt, het and hom mouse cerebella (C). (D). Relative *Oca2* abundance was reduced in the *Gabrb3* knockout mouse cerebella with varied cDNA concentrations (ng) when quantified by qRT-PCR. (E). Both *Oca2* and *Gabrb3* mRNAs were reduced in the P0 old *Gabrb3* knockout mouse eyes by qRT-PCR. (F). Relative abundance of *Gabrb3* and its flanking genes in the P0 old *Gabrb3* knockout mouse forebrains. (G). Relative abundance of the physically unrelated *Gabra1*, *Gabra3* and eye development essential factors *Mitf*, *Pax6* and *Wnt3a* in mouse forebrains of each genotype. In E and F, *p < 0.05; ** p < 0.01; *** p < 0.001 vs wt.